Asian Journal of Chemistry; Vol. 26, No. 4 (2014), 943-950

ASIAN JOURNAL OF CHEMISTRY

http://dx.doi.org/10.14233/ajchem.2014.15519

Epoxidation of Propylene Over Titanosilicate-1 in Fixed-bed Reactor: Experiments and Kinetics

LINA WANG[1,2], YAQUAN WANG[1,*], GUOQIANG WU[1], WENPING FENG[1], TENG ZHANG[1], RUMIN YANG[1], XING JIN[1], HAINAN SHI[1] and SHUHAI WANG[1]

[1]Key Laboratory for Green Chemical Technology of the Ministry of Education, School of Chemical Engineering & Technology, Tianjin University, Tianjin 300072, P.R. China
[2]Xi'an University of Science and Technology, Xi'an 710054, P.R. China

*Corresponding author: E-mail: wlnkiddy@163.com

Received: 21 March 2013; *Accepted*: 15 January 2013; *Published online*: 15 February 2014; AJC-14675

The epoxidation of propylene with hydrogen peroxide over titanosilicate-1 is studied in a fixed-bed reactor with methanol/water as the solvent. The effects of methanol concentration (40-70 wt %), hydrogen peroxide concentration (5-20 wt %), pressure (1.8-3 MPa) and temperature (35-50 °C) on the reaction are investigated. The results show that the reaction rate decreases with increasing reaction pressure, which is opposite to that reported in the literature. The activation energy of the reaction is 57.4 kJ mol^{-1} and the orders with respects to hydrogen peroxide and propylene are 0.71 and 0.29, respectively. The intrinsic kinetic modeling results show that an Eley-Rideal (H_2O_2 adsorbed) kinetic model incorporating the effects of hydrogen peroxide, propylene, methanol and propylene oxide satisfactorily agrees with the experimental results.

Keywords: Titanosilicate-1, Epoxidation, Fixed-bed reactor, Kinetic model.

INTRODUCTION

Propylene oxide, which is an essential chemical material used in the synthesis of polyether polyols, propylene glycols and propylene glycol ethers[1,2], has become increasingly important in the chemical industry since 1950s[3,4]. The global consumption of propylene oxide increased from approximately 3.9 million tons in 1991 to 6 million tons in 2009, which is predicted to grow over 7 % annually from 2009 to 2014 owing to the increasing demand[5].

Propylene oxide is currently produced by two different commercial processes, *i.e.*, the chlorohydrin process and the hydroperoxidation process[1]. However, both of these processes suffer from inevitable disadvantages. The former one is not environmentally friendly due to the utilization of environmentally hazardous chlorine and the production of chlorinated organic byproducts as well as calcium chloride. The latter process produces equimolar amounts of co-products, styrene or *tert*-butanol and the viability of this process depends on the existence of a market for such co-products. In recent years, seeking novel approaches instead of the conventional ones to produce propylene oxide has attracted worldwide attention and many studies concerning the gas-phase propylene epoxidation using molecular oxygen or the mixture of oxygen and hydrogen have been reported[6-20]. For example, Haruta *et al.*[21-26] studied the gas-phase propylene epoxidation by the mixture of oxygen and hydrogen over TiO_2, titanosilicate-1 (TS-1), Ti-MCM-41 and Ti-MCM-48 supported gold catalysts. Recently, Nguyen *et al.*[5] studied the photocatalytic epoxidation of propylene by molecular oxygen. However, the gas-phase epoxidation of propylene catalyzed by the currently available catalysts exhibited extremely low propylene oxide yield and selectivity, a considerable gap still existed between industrial applications and the fundamental academic research.

Compared to the propylene oxide production processes mentioned above, the process of epoxidizing propylene with hydrogen peroxide to propylene oxide (HPPO) catalyzed by TS-1 is advantageous in the aspects of co-products and environmental friendliness[27,28]. Figs. 1 and 2 depict the epoxidation of propylene with hydrogen peroxide over TS-1.

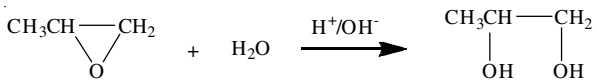

Fig. 1. Main reaction

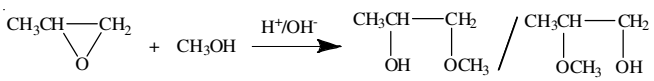

Fig. 2. Side reaction

Until now, the industrialized HPPO processes of Dow/BASF and Evonik/Uhde are the most mature, which have been commercialized in Belgium, Korea and Thailand[28-31]. A higher H_2O_2 conversion and propylene oxide selectivity can

be obtained over TS-1 or modified TS-1 using CH_3OH/H_2O as the solvent[32-35].

Previous studies[36-38] have reported the effects of solvents such as methanol/water and isopropanol and other operating conditions on the epoxidation of propylene with hydrogen peroxide. Especially, studies on the kinetics of propylene epoxidation have also been reported with slurry reactors[39,40]. Liang *et al*.[39] developed a kinetic model derived from the Eley-Rideal mechanism with H_2O_2 adsorbed on the active sites and free C_3H_6. Shin *et al*.[40] proposed a kinetic model following the Langmuir-Hinshelwood mechanism with C_3H_6 and H_2O_2 both adsorbed on the active sites. However, slurry reactors, either continuous or batch, require the separation of catalysts, suggesting extra cost and operation time with the abrasion of the catalyst. Moreover, the severe back mixing in the continuous operation and the high ratios of liquid to catalysts will lead to possible side reactions, resulting in the decrease of propylene oxide selectivity. Due to these disadvantages described above, slurry reactors are not suitable for the reaction from both the industrial and the economic points of view.

Based on the requirements and characteristics of the HPPO process and the engineering considerations, fixed-bed reactors are currently regarded more suitable. However, in contrast to the massive research on slurry reactors reported, investigations on the application of fixed-bed reactors have seldom been accessed. Pan *et al*.[41] studied the effects of operating conditions on the propylene epoxidation over TS-1 in a fixed-bed reactor and high H_2O_2 conversion (> 94 %) and propylene oxide selectivity (> 90 %) were obtained under optional conditions. Li *et al*.[42,43] reported that the supported TS-1 used in a fixed-bed reactor exhibited a long catalytic life (200 h) and the studies concerning the effects of solvents and sodium ions on the epoxidation of propylene in the fixed-bed reactor were successively reported by them. Recently, the epoxidation of propylene over modified TS-1 zeolite catalysts in a fixed-bed reactor was studied by Dong and Guo[44] and the catalytic life of the modified TS-1 was more than 1000 h with H_2O_2 conversion and propylene oxide selectivity being above 95 and 95 %, respectively. Nevertheless, modeling of hydrogen peroxide to propylene oxide over TS-1 in the fixed-bed reactor has not been explored in detail *hitherto*. Therefore, accurate understanding of the reaction kinetics is imperative in order to establish a realistic model of propylene oxide reactor for industry applications.

Thereby motivated, the present work aims to systematically examine the propylene epoxidation catalyzed by TS-1 and develop a kinetic model for a fixed-bed reactor. Continuous reactions were carried out under high-pressure and the effects of temperature, pressure, methanol concentration and hydrogen peroxide concentration on the propylene epoxidation were studied. Four kinetic models were proposed to describe the formation of propylene oxide to correlate with the experimental results to elucidate the reaction mechanism.

EXPERIMENTAL

Methanol (AR), isopropyl alcohol (AR), 30 wt and 50 wt % hydrogen peroxide (AR), tetraethyl orthosilicate (AR) and butyl titanate (AR) were purchased from Tianjin Guang fu Fine Chemical Research Institute Co., Ltd., China. Propylene (99.99 %) was purchased from Tianjin Division of SINOPEC. Silica sol was purchased from Sigma-Aldrich. Tetrapropyl-ammonium hydroxide was prepared through ion-exchange.

Synthesis of titanosilicate-1: Titanosilicate-1 was prepared according to the method described in the literature[45,46]. A solution of 2.2 g butyl titanate, 23.7 g dried isopropyl alcohol and 94.5 g tetraethyl orthosilicate were added into a solution of 15 wt % tetrapropyl-ammonium hydroxide (TPAOH) in water with vigorous magnetic stirring under N_2 atmosphere. The resulting mixture was continuously stirred for 2 h to evaporate ethanol formed. During this time, distilled water was added to compensate for the weight loss. The molar ratio of SiO_2/TiO_2 was 70 in the final solution. Then the mixture was transferred to a 300 mL PTFE lined stainless steel autoclave and heated in an oven at 175 °C, under autogenous pressure without stirring, for 72 h. After cooling to the room temperature, the crystalline product was separated from the liquid by filtration, washed with water to pH = 7, dried for 6 h at 120 °C and finally calcined for 6 h at 550 °C in air.

Synthesis of TS-1/SiO_2: TS-1/SiO_2 was prepared according to the procedure described in the literature[45]. The mixture of 1.98 g silica sol, 4 g TS-1 and 0.16 g tianqing powder was grinded for 40 min and then extruded into ϕ1 mm strips with an extrudating machine. Titanosilicate-1/SiO_2 was dried for 6 h at 120 °C and finally calcined for 6 h at 550 °C in air. The strip TS-1/SiO_2 was cut into cylindrical pieces of ϕ1 mm × 1 mm for the use in the fixed-bed reactor. In the testing to remove the internal diffusion effects, the strips were grounded into 20-40, 40-60 and 60-80 mesh.

Experimental apparatus and procedure: The schematic diagram of the experimental apparatus for the epoxidation of propylene is illustrated in Fig. 3.

8.82 g Titanosilicate-1 (15 mL) diluted with 8.55 mL ceramic particles was added into a stainless steel tube reactor (L = 1200 mm, d = 6 mm) and a little bit of stainless steel wire was put into the entrance and exit of the reactor respectively to avoid the dropping of catalysts. A stainless steel tube of 2 mm diameter with a thermocouple was embedded in the reactor to determine the temperature. The reaction temperature was controlled by a thermostatic circulating water bath with the constant flow rate of 6 L min^{-1} and the temperature difference along the reactor was less than 0.5 °C. The high pressures were realized with N_2 and the propylene was always in liquid and excess in the experiments (the molar ratios of C_3H_6/H_2O_2 were from 1.65 to 4). After the pressure reached the needed one, the flow rate of N_2 was kept at 40 mL min^{-1}. When the pressure and temperature were stabilized at the required ones, C_3H_6 (liquid) was introduced into the reactor at 0.244 mL min^{-1} by a high-pressure micro-pump, the mixed solutions of $H_2O_2/CH_3OH/H_2O$ with different flow rates were introduced into the reactor with another pump to react with C_3H_6 (30 wt % H_2O_2 in water was used to make up the mixture of $H_2O_2/CH_3OH/H_2O$ in all the experiments except the one with 70 wt % CH_3OH, which was made up by 50 wt % H_2O_2 in water. The concentration of H_2O_2 was expressed in wt % H_2O_2 in $CH_3OH + H_2O + H_2O_2$. The concentration of H_2O_2 was expressed in wt % H_2O_2 in $CH_3OH + H_2O + H_2O_2$. After reaction, the products entered the condenser with alcohols which was cooled to 2 °C. At the bottom of the apparatus, a liquid-receiver was used to collect the samples for the analysis.

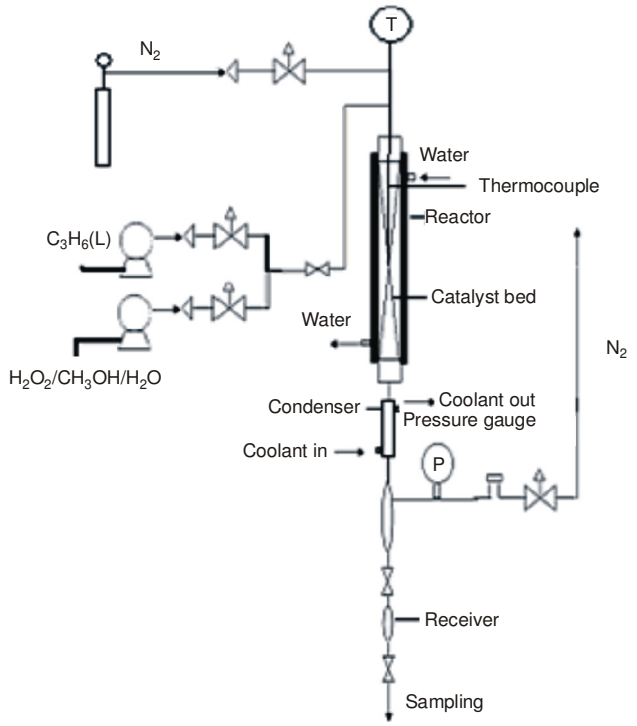

Fig. 3. Schematic diagram of experimental apparatus

The reaction was carried out at 5-10 wt % H_2O_2, 40-70 wt % CH_3OH, T = 35-50 °C, P = 1.8-3.0 MPa (N_2). During the reaction, the liquid samples were collected at given intervals (0.5 h).

Product analysis: The products of the reaction were analyzed with a HP 4890 gas chromatography (GC) equipped with a flame ionization detector (FID) and an OV-1701 (30 m × 0.25 mm × 0.33 μm) capillary column with nitrogen as the carrier gas. The unreacted H_2O_2 was measured by iodometric titration. The conversion of H_2O_2 and propylene oxide selectivity were calculated based on the starting amount of H_2O_2 according to the following two equations, respectively.

$$X_{H_2O_2} = \frac{n_{H_2O_2}^{0} - n_{H_2O_2}}{n_{H_2O_2}^{0}} \times 100\ \% \quad (1)$$

$$S_{PO} = \frac{n_{PO}}{n_{PO} + n_{MME} + n_{PG}} \times 100\ \% \quad (2)$$

$X_{H_2O_2}$ and S_{PO} denote the conversion of H_2O_2 and the selectivity of propylene oxide, respectively. n^0 and n represent the initial and the final amount in moles, respectively. MME and PG denote propylene glycol monomethyl ethers and propylene glycol, respectively.

The total reaction rate can be calculated as follows:

$$-r_{total}dV = F_{n,H_2O_2}^{0} dX_{H_2O_2} \quad (3)$$

which can be converted to

$$-r_{total}dV = F_V C_{H_2O_2}^{0} dX_{H_2O_2} \quad (4)$$

From which the total reaction rate, r_{total}, can be obtained as follows:

$$-r_{total} = C_{H_2O_2}^{0} \frac{dX_{H_2O_2}}{d(V/F_V)} \quad (5)$$

In this work, the reaction rates (r) were calculated based on the r_{total} per gram catalyst, *i.e.*,

$$r = r_{total}/m_{cat} \quad (6)$$

In repeating the experiments, it was found that both the reaction rates and the propylene oxide selectivity exhibited the errors within ±5 %.

RESULTS AND DISCUSSION

Effects of operating conditions: To avoid the formation of hot spots, the reaction has been conducted in a down-flow mode for the convenience of removing the reaction heat during reactions. In addition, the reactor was heated with circulating water, which at the same time also removes the reaction heat[47]. The temperature difference between the entry and the exit of the coolant was maintained within ± 0.5 °C to keep the reaction temperature fluctuation within a smaller range. Furthermore, small TS-1 particles (ϕ1 mm × 1 mm) was used to remove the mass and heat transfer gradients[43]. Hanika and Hajkova[48] proved that reactions with the particles of this dimension exhibited no temperature peak. And also, the catalysts were diluted with ceramic particles, which could improve the mass and heat transfer to eliminate hot spots. Therefore, it is believed that there should be no hot spots in the reaction.

In the preliminary experiments, we found that at the liquid flow rate of the mixture of $H_2O_2/CH_3OH/H_2O \geq 0.29$ mL/min, the external diffusion effect disappeared and at the catalyst particle sizes ≤ ϕ1 mm × 1 mm, the internal diffusion effect could be neglected[49]. So in the kinetic experiments, the catalyst particle sizes of ϕ1 mm × 1 mm were used and the liquid flow rates were all above 0.29 mL/min. In addition, in the testing to the decomposition of hydrogen peroxide over TS-1 at 35 to 55 °C, it was found that the decomposition of hydrogen peroxide at 35 to 50 °C was less than 6 % and could be neglected.

Effect of methanol concentration: It is known that methanol is the best among many kinds of protic or aprotic solvents for the epoxidation of propylene[27]. Therefore, methanol/water mixtures were used as the solvent and the effect of the methanol concentration on the reaction was studied.

As shown in Fig. 4, the reaction rate and propylene oxide selectivity increased with the rising methanol concentration, but did not change appreciably when the methanol concentration increased from 65 to 70 %.

On one hand, the increase of the reaction rate with increasing the methanol concentration could be attributed to the increase in the solubility of propylene in $H_2O_2/CH_3OH/H_2O$. On the other hand, the results could be also explained by the 5-membered ring mechanism of epoxidation proposed in the literature, in which the increase of the methanol concentration improved the formation rate of the 5-membered ring active adducts[27,50-52]. When the methanol concentration exceeded 65 wt %, the reaction rate did not change appreciably. The water concentration decreased with the rising methanol concentration, as a result, the side reactions were reduced and propylene oxide selectivity increased. Therefore, 65 wt % was the suitable concentration for the reaction.

Effect of hydrogen peroxide concentration: The effects of hydrogen peroxide concentration on the reaction rate and

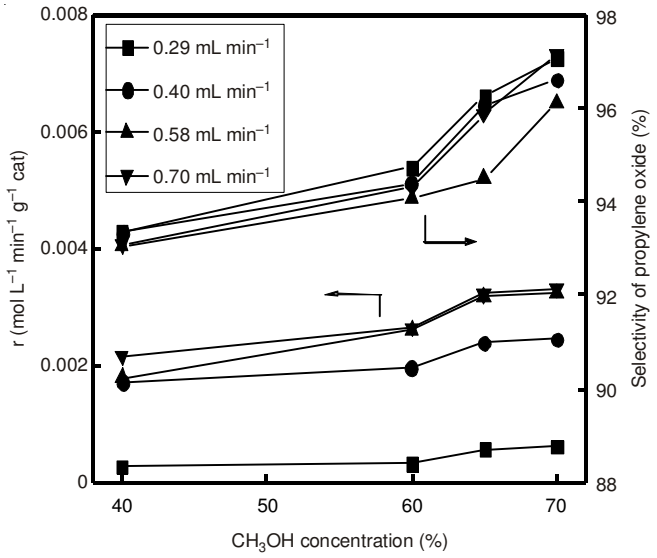

Fig. 4. Effect of methanol concentration on reaction rate and propylene oxide selectivity. Reaction conditions: T= 40 °C, P= 2.5 MPa, 10.64 wt % H_2O_2 with H_2O in balance

propylene oxide selectivity are shown in Fig. 4. The results indicated that the reaction rate increased with the rising hydrogen peroxide concentration, but propylene oxide selectivity decreased conversely.

It has been reported that the reaction order with respects to hydrogen peroxide ranged between zero and unity[39,40]. According to this conclusion, the increase of the reaction rate with the increasing hydrogen peroxide concentration shown in Fig. 5 was reasonable.

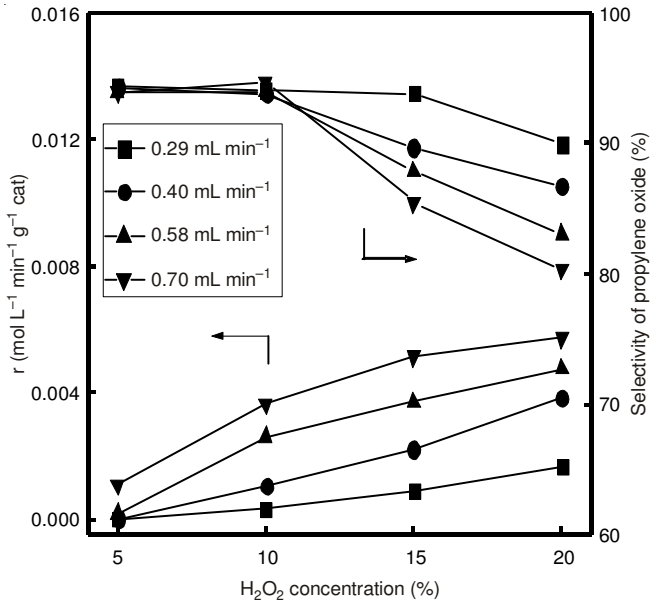

Fig. 5. Effect of hydrogen peroxide concentration on reaction rate and propylene oxide selectivity. Reaction conditions: T= 40 °C, P = 2.5 MPa, the H_2O concentration is 7/3 times the corresponding H_2O_2 concentration with CH_3OH in balance

The water concentration increased with the increasing hydrogen peroxide concentration, which accelerated the side reactions, as a result, the propylene oxide selectivity decreased. It was noteworthy that the selectivity between 10 and 20 % H_2O_2 changed significantly; indicating that side reactions were promoted at more than about 25 % H_2O_2. The order of the H_2O_2 concentration would be obtained in the following part.

Effect of pressure: The effect of pressure on the reaction is shown in Fig. 6. The reaction rate decreased with the rising pressure, but propylene oxide selectivity increased slightly. In addition, the reaction rate did not change appreciably after the pressure increased from 2.5 MPa to 3 MPa.

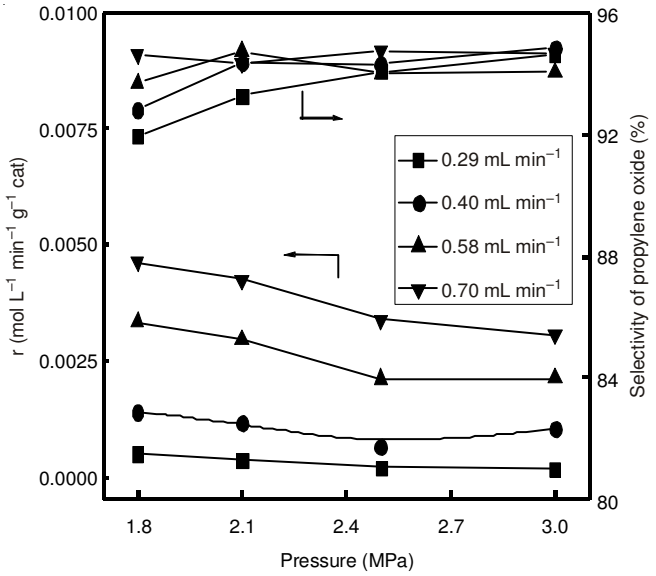

Fig. 6. Effect of pressure on reaction rate and propylene oxide selectivity. Reaction conditions: T = 40 °C, 10.64 wt % H_2O_2, 65 wt % CH_3OH, 24.36 wt % H_2O

Pan *et al.*[41] reported that the reaction rate increased with the increasing pressure in the fixed-bed reactor. However, the results obtained in this work differed from those reported markedly. The effect of pressure on the solution in liquid phase can be expressed as $(\partial \ln k/\partial p)_T = (-DV_m^{\neq})/RT$[53]. $\Delta V_m^{\neq}$ is the activation volume of the reaction, which is equal to the partial molar volume of the activated complex ($V_m^{\neq}$) minus the sum of the partial molar volume of the reactants (ΣV_{Ri}), that is, $\Delta V_m^{\neq} = V_m^{\neq} - \Sigma V_{Ri}$. Therefore, if $\Delta V_m^{\neq} > 0$, the reaction rate will decrease with the rising pressure. In the HPPO reaction, the activated complex in the reaction is believed to a 5-membered ring active adduct with a large molar volume[51], which is larger than the sum of the partial molar volume of H_2O_2 and C_3H_6. Therefore, the results that the reaction rate decreased with the rising pressure were reasonable.

Effect of temperature: The effect of the reaction temperature was studied by examining the performance of TS-1 in the temperature range of 35-50 °C. Fig. 7 showed that the reaction rate increased with the increasing temperature. However, the propylene oxide selectivity decreased, which led to the reduction of the propylene oxide production rate. Especially, when the reaction temperature increased from 45 and 50 °C, the propylene oxide selectivity changed obviously, indicating that more alkyl ether of propylene glycol was produced in this temperature range.

Reaction kinetics: Eventhough the commercial-scale propylene oxide plant based on hydrogen peroxide has been employed *hitherto*, the reaction mechanism is still controversial

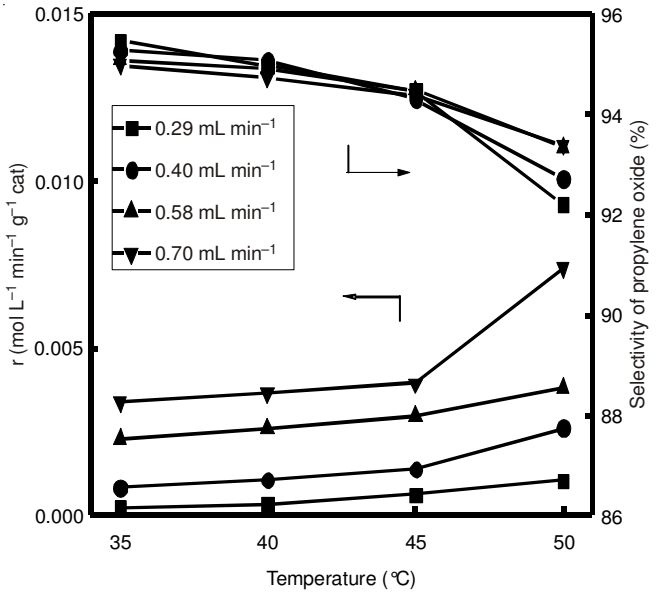

Fig. 7. Effect of temperature on reaction rate and propylene oxide selectivity. Reaction conditions: P = 2.5 MPa, 10.64 wt % H_2O_2, 65 wt % CH_3OH, 24.36 wt % H_2O

and the kinetics for fixed bed reactors has not yet been reported. Thus, the kinetics was studied below to explore the reaction in a fixed-bed reactor.

Reaction rate equation: The propylene epoxidation is a consecutive reaction, yielding propylene oxide by the reaction of propylene with H_2O_2. Therefore, the reaction rate equation could be expressed as follows:

$$r = A \times Exp.\left(-\frac{Ea}{RT}\right) \times C_{H_2O_2}{}^{\alpha} \times C_{C_3H_6}{}^{\beta}$$

Based on the experimental data of the reactions at 35 to 50 °C shown in Figs. 4-7, the rate equation was obtained by the statistical software 1STOPT and the fitting results were listed in Table-1.

TABLE-1
ESTIMATED DATA OF α, β, A, E_a

α	β	A	E_a (kJ mol^{-1})	R	F
0.71	0.29	1.87×10^7	57.4	0.962	517.6

F, Statistics and probability; R, correlation coefficient

Based on the estimation data listed in Table-1, the activation energy of the reaction was obtained as 57.4 kJ mol^{-1} and the kinetic equation (35-50 °C) was expressed as follows:

$$r = 1.87\times10^7 \times Exp.\left(-\frac{5.74\times10^4}{RT}\right) \times C_{H_2O_2}{}^{0.71} \times C_{H_3O_6}{}^{0.29}$$

It could be derived from the kinetic equation that the order of the reaction was 0.71 with respect to hydrogen peroxide, which was consistent with the result in Fig. 5.

Kinetic Model

Reaction mechanism: Owing to the formation of 5-membered rings mechanism described by Clerici *et al.*[27], the 5-membered ring intermediate among Ti active sites, H_2O_2 and alcohol was formed with the decrease of the system energy, which could account for the excellent activity of the epoxidation of propylene. Therefore, the adsorptions of methanol and hydrogen peroxide on TS-1 active sites should be taken into consideration in deducing the kinetic models. Due to the large concentration of methanol used in this experiment and its strong adsorption on TS-1 active sites, it was considered that the epoxidation occurred on TS-1 with adsorbed methanol molecules. In addition, the adsorption of H_2O molecules and the diffusion were neglected for the hydrophobicity of TS-1 and the adsorption of propylene was studied for the competitive adsorption with other reactants on Ti active sites[39]. The product propylene oxide could inhibit the epoxidation for the competitive adsorption with the reactants on Ti active sites. Judging from it, the adsorption of propylene oxide might also have its contribution to the kinetics.

Therefore, three steps including the adsorption of H_2O_2 and C_3H_6, surface reaction and desorption of propylene oxide occurred in the reaction; however, the results in the section of effect of methanol concentration and effect of hydrogen peroxide concentration showed that the rate of epoxidation was correlative to the concentration of reactants and increased with the concentration of C_3H_6 or H_2O_2, so the controlling step of the whole reaction was the surface reaction.

$$S + ROH \underset{}{\overset{K_1}{\rightleftharpoons}} S{\cdot}ROH \quad (1)$$

$$S{\cdot}ROH + H_2O_2 \overset{K_2}{\rightleftharpoons} S{\cdot}ROH{\cdot}H_2O_2 \quad (2)$$

$$S{\cdot}ROH + C_3H_6 \overset{K_3}{\rightleftharpoons} S{\cdot}ROH{\cdot}C_3H_6 \quad (3)$$

$$S{\cdot}ROH{\cdot}H_2O_2 + C_3H_6 \xrightarrow{k_1} S{\cdot}ROH{\cdot}PO + H_2O \quad (4)$$

$$S{\cdot}ROH{\cdot}PO \overset{K_4}{\rightleftharpoons} S{\cdot}ROH + PO \quad (5)$$

$$S{\cdot}ROH + C_3H_6 + H_2O_2 \xrightarrow{k_2} S{\cdot}ROH{\cdot}PO + H_2O_2 \quad (6)$$

$$S{\cdot}ROH{\cdot}C_3H_6 + S{\cdot}ROH{\cdot}H_2O_2 \xrightarrow{k_3} S{\cdot}ROH{\cdot}PO + S{\cdot}ROH + H_2O \quad (7)$$

Proposed reaction steps

Four kinetic models of the reactions were established based on the proposed mechanism above, which were in accordance with the Eley-Rideal or Langmuir Hinshelwood mechanisms[54].

(1) Eley-Rideal mechanism, H_2O_2 adsorbed, C_3H_6 free, surface reaction controlling.

$$r_2 = \frac{k_1K_2C_{H_2O_2}C_{C_3H_6}}{1 + K_1C_{CH_3OH} + K_2C_{H_2O2} + K_3C_{C_3H_6} + K_4C_{PO}}$$

(2) Eley-Rideal mechanism, C_3H_6 adsorbed, H_2O_2 free, surface reaction controlling.

$$r_1 = \frac{k_1K_3C_{H_2O_2}C_{C_3H_6}}{1 + K_1C_{CH_3OH} + K_2C_{H_2O2} + K_3C_{C_3H_6} + K_4C_{PO}}$$

(3) L-H mechanism, C_3H_6 and H_2O_2 adsorbed on the single active sites, surface reaction controlling.

$$r_3 = \frac{k_3K_2K_3C_{H_2O_2}C_{C_3H_6}}{\left(1 + K_1C_{CH_3OH} + K_2C_{H_2O_2} + K_3C_{C_3H_6} + K_4C_{PO}\right)^2}$$

(4) L-H mechanism, C_3H_6 and H_2O_2 adsorbed on different active sites, surface reaction controlling.

$$r_4 = \frac{k_4 K_2 K_3 C_{H_2O_2} C_{C_3H_6}}{(1 + K_3 C_{C_3H_6})(1 + K_1 C_{CH_3OH} + K_2 C_{H_2O_2} + K_4 C_{PO})}$$

The propylene concentration ($C_{C_3H_6}$) in the models was a function of the propylene solubility, which was related to the reaction temperatures, pressures and mass ratios of methanol/water. Therefore, according to the coefficient equation of Peng-Robinson equation, the solubility of propylene at different reaction temperatures, pressures and mass ratios of methanol/water was obtained by the software ASPEN.

Estimation of kinetic parameters: One reaction rate constant and three adsorption equilibrium constants were present in every kinetic model. The effect of temperature on the rate constant and adsorption equilibrium constants was assumed to obey with the Arrhenius equation and van't Hoff equation, respectively. Based on the experimental data of the propylene epoxidation in the fixed-bed reactor, the parameters of the models were estimated (Table-2) by the statistical software 1STOPT and the statistical results of the models were listed in Table-3.

As displayed in Table-3, the Eley-Rideal mechanism fitted the experimental data well, especially with the assumption that the epoxidation reaction took place between H_2O_2 adsorbed on Ti active sites and propylene in free state (Model 1). Model 1 exhibiting the optimal fitting result was regarded as the expected model which was consistent with the model obtained by Liang *et al.*[39] based on the results obtained in a slurry reactor.

TABLE-3
STATISTICAL RESULTS OF THE MODELS

	Model 1	Model 2	Model 3	Model 4
R	0.9642	0.9373	0.9450	0.8970
F	558.6	304.1	350.2	172.8

F, Statistics and probability; R, correlation coefficient

As shown in Model 1, although $C_{H_2O_2}$ and $C_{C_3H_6}$ existed in both the numerator and denominator of the kinetic equation, the concentrations in the denominator had less influence on the reaction rate. Therefore, the reaction rate increased with the rising reactant concentration. That was why the reaction rate would increase with the increasing CH_3OH and H_2O_2 concentrations. The existence of propylene oxide concentration in the denominator of the model equation showed the decreasing effect on the reaction. Therefore, propylene oxide should be removed from the reaction system as soon as possible in the practical process.

The reaction rate constant and equilibrium adsorption constants of the four models at 40 °C were calculated and the obtained values were summarized in Table-4.

TABLE-4
PARAMETERS OF THE FOUR MODELS AT 40 °C

	Model 1	Model 2	Model 3	Model 4
k(mol $L^{-1}g^{-1}$ cat min^{-1})	0.83	0.02	5.90	0.012
K_2 (mol L^{-1})	2.19	-	0.0001	0.64
K_3 (mol L^{-1})	17.04	0.28	2.22	27.26
K_4 (mol L^{-1})	2.01	-	0.15	0.00005

According to Model 1, the absorption equilibrium constants of H_2O_2, C_3H_6 and propylene oxide at 40 °C were K_2 = 2.19, K_3 = 17.04 and K_4 = 2.01 respectively as showed in Table-4. The values of the adsorption constants were consistent with the polarities of these species.

Simulation of the reaction using Eley-Rideal and Langmuir-Hinshelwood models: The reaction rates of epoxidation of propylene were calculated according to the estimated parameters of the four models and the calculated reaction rates were plotted against the experimental ones as shown in Figs. 8 and 9. The results showed that the experimental data satisfactorily fitted the Eley-Rideal mechanism, whereas they exhibited poor agreements with the Langmuir-Hinshelwood mechanisms.

Conclusion

Operating conditions such as methanol concentration, pressure, hydrogen peroxide concentration and reaction temperature remarkably affected the reaction rate and propylene oxide selectivity. The rates of propylene oxide production were observed to increase with the rising methanol concentration, reaction temperature and hydrogen peroxide concentration, however, decrease with the rising reaction pressure. Propylene oxide selectivity increased with the rising methanol concentration and reaction pressure, but decreased with the increasing hydrogen peroxide concentration and reaction temperature.

TABLE-2
KINETIC PARAMETERS OF VARIOUS MODELS

	Model 1	Model 2	Model 3	Model 4
K	$1.46\times10^{5}\times\exp(-\frac{3.14\times10^{4}}{RT})$	$4.17\times10^{5}\times\exp(-\frac{4.41\times10^{4}}{RT})$	$1.80\times10^{6}\times\exp(-\frac{3.29\times10^{4}}{RT})$	$1.09\times10^{5}\times\exp(-\frac{4.17\times10^{4}}{RT})$
K_2	$2.58\times10^{5}\times\exp(-\frac{3.04\times10^{4}}{RT})$	$-5.75\times\exp(\frac{-9.76\times10^{3}}{RT})$	$8.02\times10^{6}\times\exp(-\frac{6.53\times10^{4}}{RT})$	$2.81\times10^{3}\times\exp(-\frac{2.18\times10^{4}}{RT})$
K_3	$3.59\times10^{-6}\times\exp(\frac{4\times10^{4}}{RT})$	$3.42\times10^{5}\times\exp(-\frac{3.65\times10^{4}}{RT})$	$8.30\times10^{-6}\times\exp(\frac{3.25\times10^{4}}{RT})$	$2.34\times10^{2}\times\exp(-\frac{5.60\times10^{4}}{RT})$
K_4	$2.82\times10^{3}\times\exp(-\frac{1.89\times10^{4}}{RT})$	$-1.35\times10^{3}\times\exp(-\frac{2.39\times10^{4}}{RT})$	$0.04\times\exp(\frac{3.45\times10^{3}}{RT})$	$1.16\times10^{2}\times\exp(-\frac{3.80\times10^{4}}{RT})$

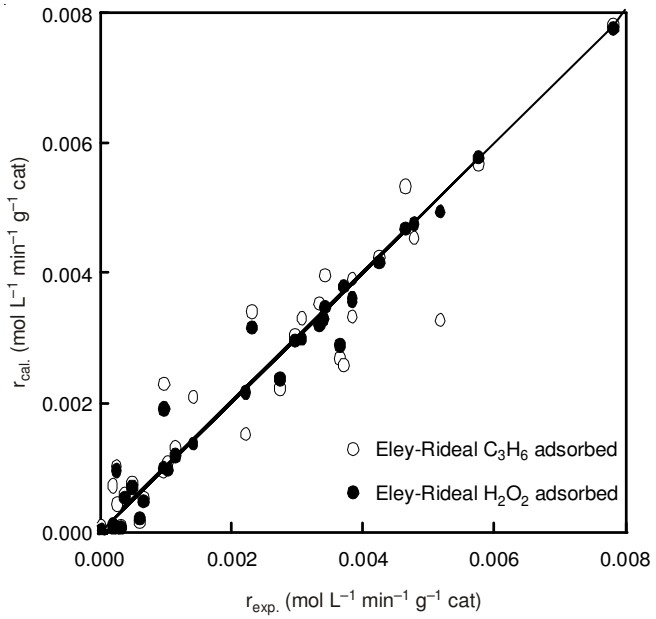

Fig. 9. Experimental rates and calculated rates according with Eley-Rideal models ($r_{exp.}$ *vs*. $r_{cal.}$)

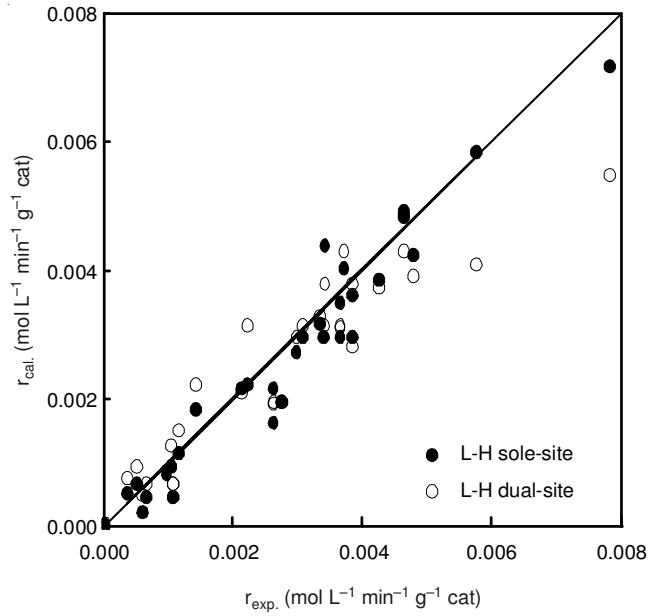

Fig. 10. Experimental rates and calculated rates according with L-H models ($r_{exp.}$ *vs*. $r_{cal.}$)

The reaction rate equation was obtained with E_a = 57.4 kJ mol^{-1} and the orders with respects to hydrogen peroxide and propylene were 0.71 and 0.29, respectively. The Eley-Rideal (H_2O_2 adsorbed) kinetic model satisfactorily predicted the experimental results and could be utilized to describe the reaction mechanism.

Nomenclature

Xi = conversion of species i (%)
n_i^0 = initial number of moles of species i (mol)
n_i = number of moles of species i (mol)
Si = selectivity to product I (%)
r_{total} = total reaction rate (mol L^{-1} min^{-1}),
r = reaction rate (mol L^{-1} g^{-1} cat min^{-1})
F^0_{n,H_2O_2} = initial flow rate of moles of H_2O_2 (mol min^{-1})
FV = flow rate of volume (L min^{-1})
V = reactor volume (L)
k_i = reaction rate constant of species i (mol $L^{-1}g^{-1}$ cat min^{-1})
K_i = adsorption equilibrium constant of species i (mol L^{-1})
α, β = orders of CH_2O_2 and CC_3H_6
A = preexponential factor (mol $L^{-1}g^{-1}$ cat min^{-1})
C_i = concentration of species i (mol kg^{-1} or mol L^{-1})
E_a = apparent activation energy of the reaction (kJ mol^{-1})
m_{cat} = catalyst mass (g)
$\Delta V_m^{\neq}$ = the activation volume of the reaction
$V_m^{\neq}$ = the molar volume of the activated complex
ΣV_{Ri} = the sum of the molar volume of the reactant i

ACKNOWLEDGEMENTS

This work has been supported by Natural Science Foundation of China with Grant No. 21276183.

REFERENCES

1. T.A. Nijhuis, M. Makkee, J.A. Moulijn and B.M. Weckhuysen, *Ind. Eng. Chem. Res*., **45**, 3447 (2006).
2. C. Neri, B. Anfossi, A. Esposito and F. Buonomo, Process for the Epoxidation of Olefinic Compounds. US Patent 4833260 (1989).
3. K. Weissermel, H.J. Arpe and C.R. Lindley, Industrial Organic Chemistry; Wiley-VCH: Weinheim (2003).
4. D. Kahlich, U. Wiechern and J. Lindner, Propylene Oxide in Ullmann's Encyclopedia of Industrial Chemistry; John Wiley & Sons Inc: Hoboken (2009).
5. V.H. Nguyen, H.Y. Chan, J.C.S. Wu and H. Bai, *Chem. Eng. J*., **179**, 285 (2012).
6. T.A. Nijhuis, B.J. Huizinga, M. Makkee and J.A. Moulijn, *Ind. Eng. Chem. Res*., **38**, 884 (1999).
7. R. Meiers and W.F. Holderich, *Catal. Lett*., **59**, 161 (1999).
8. G. Jenzer, T. Mallat, M. Maciejewski, F. Eigenmann and A. Baiker, *Appl. Catal. A*, **208**, 125 (2001).
9. A.K. Sinha, S. Seelan, S. Tsubota and M. Haruta, *Top. Catal*., **29**, 95 (2004).
10. N. Yap, R.P. Andres and W.N. Delgass, *J. Catal*., **226**, 156 (2004).
11. A.K. Sinha, S. Seelan, M. Okumura, T. Akita, S. Tsubota and M. Haruta, *J. Phys. Chem. B*, **109**, 3956 (2005).
12. J.L. Zhao, J.C. Zhou, J. Su, H.C. Guo, X.S. Wang and W.M. Gong, *AIChE J*., **53**, 3204 (2007).
13. Z.H. Suo, M.S. Jin, J.Q. Lu, Z.B. Wei and C. Li, *J. Nat. Gas Chem*., **17**, 184 (2008).
14. T. Liu, P. Hacarlioglu, S.T. Oyama, M.F. Luo, X.R. Pan and J.Q. Lu, *J. Catal*., **267**, 202 (2009).
15. H.W. Yang, D.L. Tang, X.N. Lu and Y.Z. Yuan, *J. Phys. Chem. C*, **113**, 8186 (2009).
16. G.W. Zhan, M.M. Du, D.H. Sun, J.L. Huang, X. Yang, Y. Ma, A.R. Ibrahim and Q.B. Li, *Ind. Eng. Chem. Res*., **50**, 9019 (2011).
17. J.H. Huang, E. Lima, T. Akita, A. Guzman, C.X. Qi, T. Takei and M. Haruta, *J. Catal*., **278**, 8 (2011).
18. G.W. Zhan, M.M. Du, J.L. Huang and Q.B. Li, *Catal. Commun*., **12**, 830 (2011).
19. J. Su, J.C. Zhou, C.Y. Liu, X.S. Wang and H.C. Guo, *Chin. J. Catal*., **31**, 1195 (2010).
20. M.M. Du, G.W. Zhan, X. Yang, H.X. Wang, W.S. Lin, Y. Zhou, J. Zhu, L. Lin, J.L. Huang, D.H. Sun, L.S. Jia and Q.B. Li, *J. Catal*., **283**, 192 (2011).
21. B.S. Uphade, M. Okumura, S. Tsubota and M. Haruta, *Appl. Catal. A*, **190**, 43 (2000).
22. A.K. Sinha, S. Seelan, T. Akita, S. Tsubota and M. Haruta, *Appl. Catal. A*, **240**, 243 (2003).
23. C.X. Qi, T. Akita, M. Okumura, K. Kuraoka and M. Haruta, *Appl. Catal. A*, **253**, 75 (2003).

24. J. Huang, T. Takei, T. Akita, H. Ohashi and M. Haruta, *Appl. Catal. B*, **95**, 430 (2010).
25. C.X. Qi, J.H. Huang, S.Q. Bao, H.J. Su, T. Akita and M. Haruta, *J. Catal*., **281**, 12 (2011).
26. J. Huang, E. Lima, T. Akita, A. Guzmán, C. Qi, T. Takei and M. Haruta, *J. Catal*., **278**, 8 (2011).
27. M.G. Clerici, G. Bellussi and U. Romano, *J. Catal*., **129**, 159 (1991).
28. F. Cavani and J.H. Teles, *Chem. Sus. Chem*., **2**, 508 (2009).
29. G.F. Thiele and E. Roland, *J. Mol. Catal. Chem*., **117**, 351 (1997).
30. J.H. Teles, A. Rehfinger, P. Bassler, A. Wenzel, N. Rieber and P. Rudolf, Method for the production of propylene oxide. US Patent 6756503, (2004).
31. M.G. Clerici, *Oil Gas Eur. Mag.*, **32**, 77 (2006).
32. S. Park, K.M. Cho, M.H. Youn, J.G. Seo, S.H. Baeck, T.J. Kim, Y.M. Chung, S.H. Oh and I.K. Song, *Catal. Lett*., **122**, 349 (2008).
33. G. Paparatto, A. Forlin and P. Tegon, Process for the Preparation of Olefin Oxides, US Patent 7442817 (2008).
34. V. Arca, A. Boscolo Boscoletto, N. Fracasso, L. Meda and G. Ranghino, *J. Mol. Catal. Chem*., **243**, 264 (2006).
35. W.G. Cheng, X.S. Wang, G. Li, X.W. Guo and S.J. Zhang, *J. Catal*., **255**, 343 (2008).
36. X.W. Liu, X.S. Wang, X.W. Guo and G. Li, *Catal. Today*, **93-95**, 505 (2004).
37. G. Li, J. Meng, X. Wang and G. Xinwen, *React. Kinet. Catal. Lett*., **82**, 73 (2004).
38. Z.G. Zhang, J.N. Kang and Y. Wang, *React. Kinet. Catal. Lett*., **92**, 49 (2007).
39. X.H. Liang, Z.T. Mi, Y.L. Wu, L. Wang and E.H. Xing, *React. Kinet. Catal. Lett*., **80**, 207 (2003).
40. S.B. Shin and D. Chadwick, *Ind. Eng. Chem. Res*., **49**, 8125 (2010).
41. S.C. Pan, Z. Tang, T.S. Tao and Y.Y. Feng, *Adv. Fine Petrochem*., **2**, 38 (2001).
42. G. Li, X.S. Wang, H.S. Yan, Y.Y. Chen and Q.S. Su, *Appl. Catal. A*, **218**, 31 (2001).
43. G. Li, X. Wang, H. Yan, Y. Liu and X. Liu, *Appl. Catal. A*, **236**, 1 (2002).
44. Y. Dong and X. Guo, *Acta Petrol. Sin*., **26**, 677 (2010).
45. M. Taramasso, G. Perego and B. Notari, Preparation of porous crystalline synthetic material comprised of silicon and titanium oxides, US Patent 4410501 (1983).
46. D.P. Serrano, R. Sanz, P. Pizarro, I. Moreno, P. de Frutos and S. Blázquez, *Catal. Today*, **143**, 151 (2009).
47. H. Thomas, H. Willi, T. Georg and S. Joerg, Process for the epoxidation of olefins, Eur. Patent 1247805 (2002).
48. J. Hanika and A. Hajkova, *Chem. Prum*., **37**, 398 (1987).
49. H. Liu, G.Z. Lu, Y.L. Guo, Y. Guo and J.S. Wang, *Chem. Eng. J*., **116**, 179 (2006).
50. G.N. Vayssilov, *Catal. Rev., Sci. Eng*., **39**, 209 (1997).
51. G. Bellussi, A. Carati, M.G. Clerici, G. Maddinelli and R. Millini, *J. Catal*., **133**, 220 (1992).
52. P.E. Sinclair and C.R.A. Catlow, *J. Phys. Chem. B*, **103**, 1084 (1999).
53. M.G. Evans and M. Polanyi, *Trans. Faraday Soc*., **31**, 875 (1935).
54. R.H. Perry and D.W. Green, Perry's Chemical Engineers' Handbook; McGraw-Hill: New York (2007).